

Photochemical & Photobiological Sciences

Accepted Manuscript



This is an *Accepted Manuscript*, which has been through the Royal Society of Chemistry peer review process and has been accepted for publication.

Accepted Manuscripts are published online shortly after acceptance, before technical editing, formatting and proof reading. Using this free service, authors can make their results available to the community, in citable form, before we publish the edited article. We will replace this *Accepted Manuscript* with the edited and formatted *Advance Article* as soon as it is available.

You can find more information about *Accepted Manuscripts* in the [Information for Authors](#).

Please note that technical editing may introduce minor changes to the text and/or graphics, which may alter content. The journal's standard [Terms & Conditions](#) and the [Ethical guidelines](#) still apply. In no event shall the Royal Society of Chemistry be held responsible for any errors or omissions in this *Accepted Manuscript* or any consequences arising from the use of any information it contains.



Journal Name

ARTICLE

Luminescent zinc metal-organic framework (ZIF-90) for sensing metal ions, anions and small molecules

C. Liu and B. Yan*

Received 00th January 20xx,
Accepted 00th January 20xx

DOI: 10.1039/x0xx00000x

www.rsc.org/

We synthesize a zinc zeolite-typed metal-organic framework of zeolitic imidazolate framework (ZIF-90), which exhibits an intensive blue luminescence excited under visible light. Luminescent studies indicate that ZIF-90 could be an efficient multifunctional fluorescence material for high sensitivity sensing of metal ions, anions and organic small molecules, especially for Cd^{2+} , Cu^{2+} , CrO_4^{2-} and acetone. The luminescence intensity of ZIF-90 increases with the concentration of Cd^{2+} and decreases proportionally with the concentration of Cu^{2+} , while the same quenched experimental phenomena appear in the sensing of CrO_4^{2-} . And with the increase of amount of acetone, the luminescence intensity decreases gradually in the emulsions of ZIF-90. The mechanism of the sensing properties are studied in detail as well. This studies show that the ZIF-90 could be a useful luminescent sensor for metal ions, anions and organic small molecules.

Introduction

As a new kind of micro/mesoporous material, metal organic frameworks (MOFs) have been gotten much more attentions.¹ MOFs can be readily self-assembled between metal ions/clusters and organic ligands by the coordinated interactions. And this interesting architectural form makes them structural rigidity, high porosity, and well-defined topology. These characteristics demonstrate that MOFs have a variety of potential applications, such as gas storage/separations,^{2,3} catalysis,⁴ magnetism,⁵ and sensing.^{6,7}

With the evolution of modern industry and society, chemical pollutions, such as heavy metal ions, anions and organic small molecules, are both gradually released from industrial and human activities, which are not of benefit to the sustainability of human and environment.⁸ So it is necessary to identify and monitor these environmental pollution levels directly. These detections are based on the development of advanced materials which are used mainly for recognising and sensing of harmful substances. The sample recognition cases that are putting guest molecules into the interior of host materials, as a useful sensor, the host needs bind to the distinctive guest molecule in preference to other competing species and it must register the binding event in an appropriate form.⁹ Moreover, to avoid extensive structural collapse, the chemical and

thermal stability of the host materials are necessary. In order to meet the above requirements of the host materials, porous MOFs become an appropriate choice for molecular sensing.

To build efficient porous sensors, the primary manner is to remove the excess solvent molecules in channel and pore of the synthesized-MOFs. And the choice of organic ligands with multiple coordination sites, the structural strength of the frameworks become the keys to obtain a series of suitable MOFs for molecular sensing. On this basis, the porous lanthanide MOFs (Ln-MOFs) are the main materials which are to design and synthesize for sensing applications. In particular, MOFs (*i.e.* MIL-124,¹⁰ MIL-121,¹¹ and MIL-53 COOH(Al)¹²) are applied to post-synthesize or ion-exchange with lanthanide (such as Eu^{3+}) as templates reported by our group, which display attractive sensing of metal ions, anions, and organic small molecule, respectively. Their sensing functionalities rely on the channel/pore and metal/ligand uncoordinated sites within Ln-MOFs, like metal ions contest coordinated sites with Eu^{3+} for sensing of $\text{Fe}^{2+}/\text{Fe}^{3+}$, and ions sensitize ligand to enhance luminescence for Ag^+ . Because Ln-MOFs which possess the features of lanthanide luminescence display sharp and characteristic emissions and long luminescent lifetimes.¹³ Ln-MOFs have special luminescent mechanism which happens in the progress of ligand to metal energy transfer (LMET).¹⁴ The interactions between substrate and metal or substrate and ligand can be used to tune Ln-MOFs emission intensities. Meanwhile, a series of transition metal-MOFs have reported in the papers which are based on the luminescence of ligands or ligand to metal, such as the Cd and Zn. In part, transition metal-MOFs can be used for molecular sensing, like $\text{Cd}_3(\text{TPT})_2(\text{DMF})_2$ for sensing of nitroaromatic¹⁵ and the sensing of acetone in $\text{Zn}(\text{MeIM})$.¹⁶

* Address here.

* Address here.

* Address here.

† Footnotes relating to the title and/or authors should appear here.

Electronic Supplementary Information (ESI) available: [details of any supplementary information available should be included here]. See DOI: 10.1039/x0xx00000x

The above works are mainly concerned on the choice and design to synthesize different luminescent MOFs which could provide capably potential space within channel/pore or coordination sites for molecular sensing. Most luminescent MOFs have the flexible uncoordinated carboxylate ligands for molecular sensing. Like carboxylate ligands, nitrogen sites within imidazole make them have the capability to selective sense with metal ions.¹⁷ However, metal imidazolate frameworks have rarely been studied deeply. As a subfamily of metal organic frameworks, porous zeolitic imidazolate framework (ZIFs)¹⁸ with exceptional chemical and thermal stability are expected to play roles in recognition of molecules. Zn(ICA)₂(DMF)(H₂O)₃¹⁹ (ZIF-90, ICA = imidazolate-2-carboxyaldehyde), the structure is related to the sodalite topology (SiO₂, SOD) by replacing the Si and O with Zn(II) and ICA ligands, respectively. The expanded 3D ZIF structure have high enough porosity with an aperture of 3.5 Å in diameter and a pore size of 11.2 Å to recognise molecules readily. And the ligand of ICA which not only have the nitrogen sites within imidazolate but also have uncoordinated aldehyde group, make ZIF-90 has the ability to sense selectively with metal ions. With all the features, ZIF-90 can be assumed to play an efficient porous sensors in sensing study.

Herein we synthesize ZIF-90 and explore its sensing property for metal ions, anions and organic small molecules. The changed fluorescence of the desolvated ZIF-90 with various ions and molecules and the mechanism of the sensing properties are studied in detail as well.

Results and discussion

Characterization

The structure of ZIF-90 is identical to the SOD topology and have high enough porosity with an aperture of 3.5 Å and a pore size of 11.2 Å. As shown in Figure S1, the powder X-ray diffraction (PXRD) patterns of as-synthesized ZIF-90 and desolvated ZIF-90 (ZIF-90a) both are almost similar to the bottom of simulated ZIF-90, indicating that the structure accords with the literature reported and the basic 3D framework is retained, respectively. This porous material are obtained by removing the excess solvent molecules within the pore and skeleton and thermal activated for subsequent appliions. Meanwhile the thermal stability of the porous material is examined by thermal gravity analysis (TGA) measurements which was performed under air with a heating rate of 5 k·min⁻¹ (Figure 1). TGA data indicates that ZIF-90 releases its internal DMF molecules in the temperature range between 25 °C and 300 °C to get its desolvated powder ZIF-90a which structure collapse starts from 400 °C. TGA reveals the high thermal stability of ZIF-90a 3D frameworks. Figure S2 presents the N₂ adsorption - desorption isotherms of ZIF-90. This sample unlike a type I adsorption curve which commonly was seen in microporous materials, can be observed typical type IV curves with a hysteresis loops behaviour. The atypical hysteresis of these N₂ adsorption isotherms could be ascribed to the steric hindrance of the free uncoordinated aldehyde groups within the channels, which reduce the access of N₂ molecules. The Langmuir surface area is 829.2341 m²·g⁻¹, which is in reasonable close to the value reported by Omar M. Yaghi *et al.*¹⁹

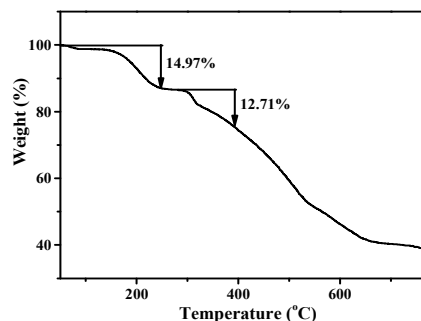


Figure 1 TGA trace of compound ZIF-90.

Luminescent properties

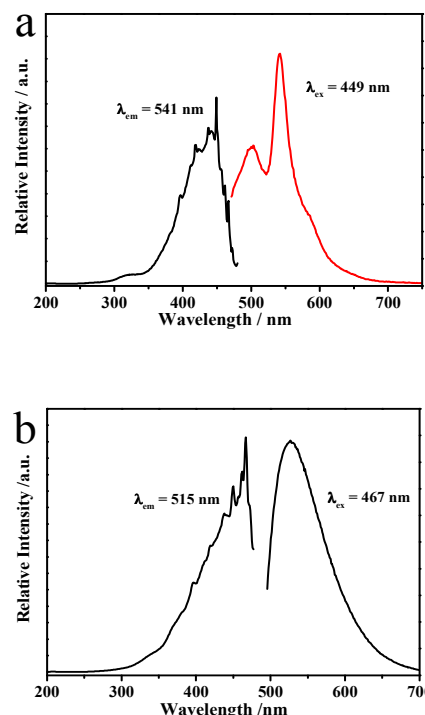


Figure 2 a) the excitation ($\lambda_{ex} = 449$ nm) and emission spectra ($\lambda_{em} = 541$ nm) of imidazolate-2-carboxyaldehyde (ICA), and b) the as-synthesized ZIF-90 ($\lambda_{ex} = 467$ nm and $\lambda_{em} = 515$ nm).

The solid-state excitation and emission spectra of the skeleton ligand imidazolate-2-carboxyaldehyde (ICA) and the porous material ZIF-90 have been studied at room temperature (Figure 2). The emission spectrum of ICA shows a main peak with a max value at 541 nm under excited at 449 nm, and the $\pi^*-\pi$ transition of ICA give rise to this emission (Figure 2a).²⁰ In the Figure 2b, when monitored by the emission wavelength at 476 nm, the excitation spectrum displays the maximum peak at 515 nm. It is known that ZIFs which have transition-metal ions without unpaired electrons (such as Zn²⁺-like has d¹⁰ formations),¹⁶ can gain linker-based highly emissive materials. The luminescent behaviour of ZIF-90 is probably linker-based because the emission is in the region of the free ligand ICA (emission at 541 nm). The blue shift (515 nm for ZIF-90) is

probably related to the coordination effect of free ICA to the Zn^{2+} . The emission peaks of ZIF-90a1 which are diffused into the solutions of different metal ions (Cd^{2+} , Ca^{2+} , Mn^{2+} , Hg^{+} , Co^{2+} , Ni^{2+} , or Cu^{2+}), ZIF-90a2 with anions (NO_3^- , $C_2O_4^{2-}$, CO_3^{2-} , Br^- , F^- , Cl^- , I^- , PO_4^{3-} , CrO_4^{2-} , HCO_3^- , NO_2^- and S^{2-}) and ZIF-90a3 with organic small molecules (formamide, ethylenediamine, dimethyl formamide, acetonitrile, diethyl ether, acetone, methanol and ethanol) are almost similar to the photoluminescence spectra of as-synthesized ZIF-90 (all the emission peak almost located at about 515 nm). The main structure of the ZIF-90 framework are not changed, collapsed or destroyed by the various metal ions, anions and organic molecules when these introduce into the 3D channel. The ZIF-90a1, ZIF-90a2 and ZIF-90a3 are centrifuged after luminescence measurement, washed three times and dried under vacuum for 5 h at 100 °C to obtain there powders, respectively.

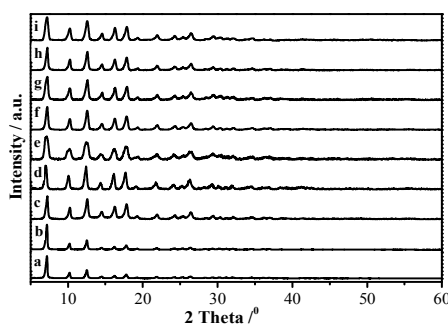


Figure 3 Powder X-ray diffraction patterns of a) simulated ZIF-90, b) as-synthesized ZIF-90 and ZIF-90 after the introduction of various metal ions: c) Cd^{2+} , d) Ca^{2+} , e) Mn^{2+} , f) Hg^{+} , g) Co^{2+} , h) Ni^{2+} , and i) Cu^{2+} .

The PXRD patterns of ZIF-90a1 powders are also identical to that of ZIF-90 (Figure 3), which suggests that the crystal lattice remains robust after the diffusion. The PXRD of ZIF-90a2 and ZIF-90a3 are listed in the Figure S3 and S4. All the PXRD patterns can prove the high stability of the 3D network of porous ZIF-90.

Sensing of metal ions

In consideration of the excellent luminescence and good stability of ZIF-90, we examine the potential application of ZIF-90 for detecting metal ions. The desolvated sample (ZIF-90a) was simply immersed in an aqueous solution of 10^{-2} M MCl_x ($M = Cd^{2+}$, Ca^{2+} , Mn^{2+} , Hg^{+} , Co^{2+} , Ni^{2+} , and Cu^{2+} , respectively). The luminescent properties were recorded and compared in Figure S5. The results revealed that various metal ions display markedly different effects on the luminescence of ZIF-90a.

For example, the luminescence intensity at 515 nm is decreased compared with H_2O when Ca^{2+} , Mn^{2+} , Hg^{+} , Co^{2+} , Ni^{2+} , and Cu^{2+} are introduced. In the contrast, the luminescence intensity of ZIF-90a1 is largely dependent on the metal ions solutions, such as the interaction with Cd^{2+} drastically enhanced and Cu^{2+} quenched the luminescence intensity. The rest of the metal ions (Ca^{2+} , Mn^{2+} , Hg^{+} , Co^{2+} and Ni^{2+}) did not cause any significant change to the intensity of the ZIF-90a luminescence. The luminescence intensity of the ZIF-90a1 interacting with different metal ions in 10^{-2} M aqueous solution of MCl_n shows in Figure 4.

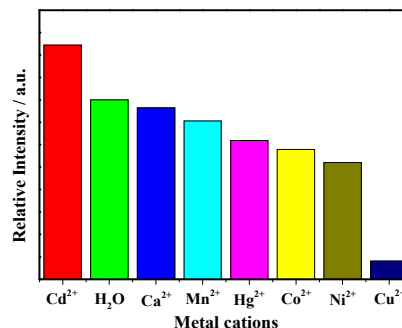


Figure 4 the luminescence intensity of the ZIF-90a1 interacting with different metal ions in 10^{-2} M aqueous solution of MCl_n (excited monitored at 476 nm).

ZIF-90a was immersed in Cd^{2+} solutions containing different concentrations of $CdCl_2$ for further luminescence studies, and the emission spectra of ZIF-90a in the presence of various concentrations of Cd^{2+} aqueous solutions under excited at 476 nm shows in Figure 5. As we observed, the change of luminescence intensity of the ZIF-90a/ Cd^{2+} is consistent with the concentration of the metal ion. The luminescence intensity increases with the concentration of Cd^{2+} from 0 to 500 μ M. The luminescence intensity of the ZIF-90a/ Cd^{2+} is about three times compared 500 μ M solution of $CdCl_2$ with the pure of ZIF-90a, that can indicate the potential sensing of ZIF-90a for Cd^{2+} ion.

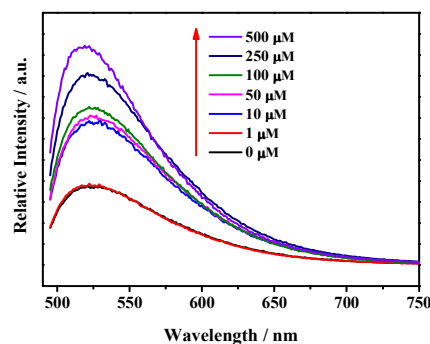


Figure 5 Emission spectra of ZIF-90a in aqueous solutions in the presence of various concentrations of Cd^{2+} under excited at 476 nm.

To illustrate the mechanism of Cd^{2+} sensing, the FTIR and EDS spectra were obtained before and after Cd^{2+} diffusion. Figure 6 indicates the FTIR spectra of ZIF-90a and ZIF-90a/ Cd^{2+} materials. The primary peaks match well with previously reported results. The spectra of ZIF-90a before and after sensing are similar except for some new peaks. The broad peak at 3500 cm^{-1} is ascribed to the stretching vibration of hydroxyl and amino groups, which are difficult to distinguish and separate completely. The intense peak at 1024 cm^{-1} is attributed to the stretching vibration of Cd–O, indicating the successful sensing of Cd^{2+} species onto ZIF-90. The absorption peak at 500 cm^{-1} is characterized by metal–oxygen vibration. The scanning electron microscope (SEM) and energy dispersive spectrometer (EDS) analysis of the ZIF-90a/ Cd^{2+} (Figure S6) reveal that some Cd^{2+} are detected on the surface after diffusion, and the weight percent and atomic percent of elements

in the ZIF-90a/Cd²⁺ (Table S1), confirming the successful sensing of Cd²⁺.

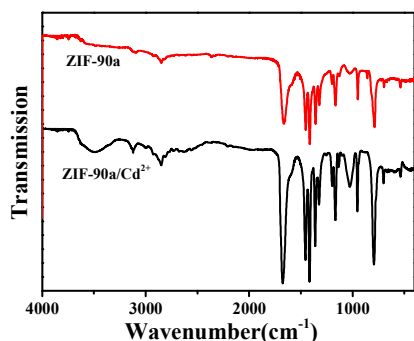


Figure 6 FTIR spectra of ZIF-90a before and after Cd²⁺ sensing.

On the contrary, the luminescence intensity of ZIF-90a decreases with the concentration of Cu²⁺ and the emission spectra of ZIF-90a/Cu²⁺ in various concentrations of Cu²⁺ solutions displays in Figure S7. The luminescence intensity of the ZIF-90a/Cu²⁺ is also identical to the concentration of the metal ion. The luminescence intensity of the ZIF-90a/Cu²⁺ is about quarter from 500 μM solution of CuCl₂ to that of ZIF-90a, illustrating ZIF-90a possess the ability of sensing for Cu²⁺ ion. The mechanism of the quenching effect between ZIF-90a and Cu²⁺ that would be a weak atomic interactions of imidazole nitrogen atoms and a coordination of aldehyde group of ICA to Cu²⁺ in the ZIF-90a/Cu²⁺, such binding reduces the intraligand luminescent efficiency and results in the quenching effect.³³ The forceful enhancing effect of Cd²⁺ and the quenching effect of Cu²⁺ to ZIF-90a provide a practical application for developing sensing materials.

In addition, the enhancing and quenching effects of metal ions on the luminescence of ZIF-90a were evaluated by the fluorescence decay time. As shown in Table S2, most of the metal ions have no significant effects on the luminescence lifetime of ZIF-90a, while Cd²⁺ and Cu²⁺ ions exhibit varying degrees of increase/decrease in the luminescence lifetimes which displays 315.51 μs and 128.71 μs, which is in agreement with the variation of the luminescence intensity. This observation agrees well with the responses of luminescence of ZIF-90a towards various metal ions.

Sensing for anions and organic small molecule

Simultaneously, various anions were selected to study the sensing function of anions by diffusing a certain amount of ZIF-90a in different anions aqueous solutions (anions = NO₃⁻, C₂O₄²⁻, CO₃²⁻, Br⁻, F⁻, Cl⁻, I⁻, PO₄³⁻, CrO₄²⁻, HCO₃⁻, NO₂⁻ and S²⁻). The PXRD can confirm that ZIF-90a framework almost kept unchanged (Figure S3). The luminescent measurements illustrate that the difference anions have a great influence in the luminescence intensity of ZIF-90a as shown in Figure S8. Remarkably, CrO₄²⁻ has the largest quenching effect on the luminescent emission and has reduced the luminescent lifetime of ZIF-90a (Figure S9).

To research the luminescence quenching reason of CrO₄²⁻, concentration-based studies in the luminescence properties of ZIF-90a were carried out under the existence of CrO₄²⁻ ion. The luminescence of ZIF-90a was gradually quenched with the CrO₄²⁻ concentration increased (Figure 7). The emission intensity of the

ZIF-90a emulsion declines sharply with the increase of CrO₄²⁻ concentration from 0 to 500 μM. Quantitatively, this quenching effect can be rationalized by the Stern-Volmer equation:³⁹

$$I_0/I = 1 + K_{sv}[M]$$

The values of I₀ and I are the luminescence intensity of the ZIF-90a emulsion and ZIF-90a/CrO₄²⁻, respectively. K_{sv} is the quenching constant, [M] is the concentration of CrO₄²⁻. On the basis of the experimental data illustrating in the inset of Figure 7, in the K_{sv} curve of ZIF-90a with CrO₄²⁻, the linear correlation coefficient (R) is 0.99909, which suggests that the quenching effect of CrO₄²⁻ on the luminescence of ZIF-90a agrees the Stern-volmer mode well. The K_{sv} value is calculated as 5.03×10³, which reveals a strong quenching effect on the ZIF-90a luminescence.

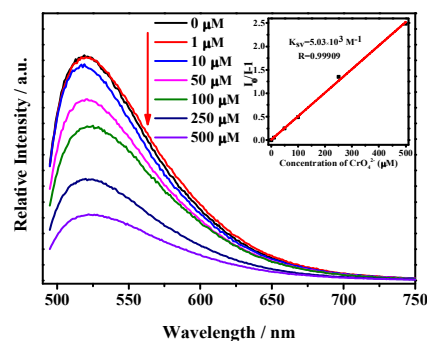


Figure 7 Emission spectra of ZIF-90a/CrO₄²⁻ in aqueous solutions in the presence of various concentrations of CrO₄²⁻ under excitation at 476 nm and the inset is the K_{sv} curve of ZIF-90a/CrO₄²⁻.

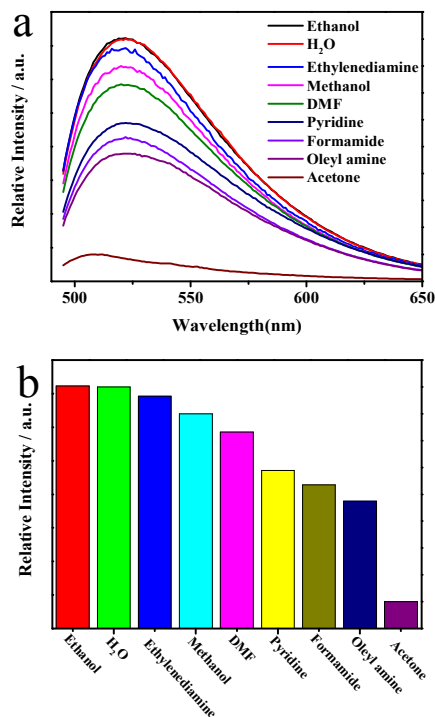


Figure 8 a) the photoluminescence spectra of ZIF-90a (3 mg) dispersed into different organic small molecules (3 ml), b) the luminescence intensity of the ZIF-90a3 interacting with different organic small molecules solution (excited monitored at 476 nm).

In addition, we also explore the sensing function of ZIF-90a for organic small molecules because of their environmental biological hazards. The PXRD patterns of ZIF-90a3 illustrate good stability treated by different organic small molecules, before the luminescent measurements (Figure S4). As shown in Figure 8, the luminescence spectra are significantly dependent on the organic molecules, particularly in the case of acetone, which exhibit clearly quenching effects. When diffusing a certain amount of ZIF-90a (3 mg) in different quantities (1-5 ml) of acetone to obtain an emulsion, the emission of ZIF-90a3 shows a dramatic decreased luminescence intensity (Figure S10).

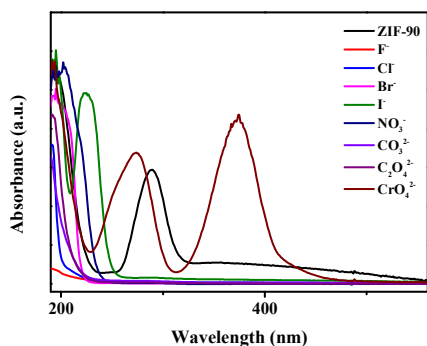


Figure 9 UV-vis absorption spectra of suspended ZIF-90 in H₂O solution compared to the different anions (F⁻, Cl⁻, Br⁻, I⁻, NO₃⁻, CO₃²⁻, C₂O₄²⁻ and CrO₄²⁻) dissolved in H₂O solution.

Until now, the mechanisms for such quenching effects of anions and small solvent molecules are still not very clear. To deeply understand the luminescence quenching effects by CrO₄²⁻, the UV-vis spectra of anions themselves are measured (Figure 9). It is obvious that the absorption peak of ZIF-90a is almost overlapped by the absorption of CrO₄²⁻. The CrO₄²⁻ competes the absorption of light energy with the organic ligand and hence reduces the amount of light absorbed by the ligand thereby reducing the efficiency of energy transfer from the ligand to the metal ions of the frameworks. The luminescent signal induced by organic small molecules can be partially attributed to the UV-vis absorption (Figure S11). The result indicates that the absorption band of acetone partially overlaps with the absorption band of ZIF-90a which has reduced the absorption of light by organic ligand and affected the energy transformation.

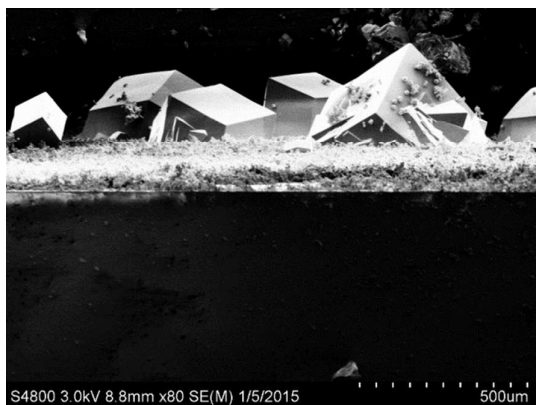


Figure 10 the cross section SEM images of the ZIF-90 membrane supported on the APTES modified ITO surface.

We used the APTES to modify the surface of the ITO and synthesized the ZIF-90 membrane on the surface (Figure 10). Scanning electron microscopy (SEM) shows the morphology of ZIF-90 membrane (cross section). Next, we will attempt to prepare the membrane on the soft material surface to study the gas detection. And we will develop a fluorescence ZIF-90 test paper for rapid detection of ions to make the detection simple and portable.

Experimental

Materials and general procedures All reagents were obtained from commercial sources (Aladdin, Sinoreagent, Sigma Aldrich) and unless otherwise stated were used without further purification.

Synthetic procedure for zeolitic imidazolate frameworks (ZIF-90)²¹ As-synthesized ZIF-90, 1 mL trimethylamine (TEA) was dissolved into a 25 mL beaker with 10 mL n-hexane (A); in a 250 mL beaker, 0.1 g Zn(NO₃)₂·6H₂O and 0.06 g imidazolate-2-carboxyaldehyde (ICA) were dissolved in 40 mL DMF (B), after stirred for 30 min, A was dropped into B slowly. White precipitate appears immediately at the interface between n-hexane and DMF. After aging for 4 h, the white precipitate was collected and washed three times with DMF and chloroform, respectively. To obtain ZIF-90a (desolvated ZIF-90 denoted as ZIF-90a), the product was activated with chloroform (3 × 10 mL) over a three-day period before being dried under vacuum for 10 h at 130 °C (yield: 0.08 g, 75% based on ICA).

pH-stability studies²² 25 mg of ZIF-90a was diffused into 50 mL deionized water and treated for 10 min by ultrasonic. 2 mL of the above solution was added to the tubes containing 8 mL of deionized water in the range of pH from 1.0 to 14.0 (adjusted using HCl or NaOH). The fluorescence spectra were recorded after 5 min of equilibration time in the cuvettes.

Luminescent measurements The photoluminescence properties of ZIF-90a in various metal ions, anions and organic solvent solutions (denoted as ZIF-90a1, ZIF-90a2 and ZIF-90a3, respectively) were investigated at room temperature. For the properties of sensing with respect to metal ions, the emulsion of ZIF-90a1 was obtained by diffusing ZIF-90a powder (3.0 mg) into deionized water solution (3.0 mL) of MCl_x (M = Cd²⁺, Ca²⁺, Mn²⁺, Hg⁺, Co²⁺, Ni²⁺ or Cu²⁺) under the concentrations of 10⁻² M. The emulsion of ZIF-90a2 was prepared by dispersing ZIF-90a powder (3.0 mg) into deionized water solution (3.0 mL) of KxN1 (N1 = NO₃⁻, C₂O₄²⁻, CO₃²⁻, Br⁻, F⁻, Cl⁻, I⁻, PO₄³⁻ or CrO₄²⁻) and NaxN2 (N2 = HCO₃⁻, NO₂⁻ or S²⁻) at the same concentrations. The ZIF-90a3 emulsions were prepared by introducing 3.0 mg of ZIF-90a powder into 3.0 mL of formamide, ethylenediamine, dimethyl formamide, acetonitrile, diethyl ether, acetone, methanol and ethanol, respectively. After sonicated for 10 min, the fluorescence spectra were measured.

Synthesis of ZIF-90 membrane

APTES modification on the ITO surface

²³

In order to make 3-aminopropyltriethoxysilane (APTES) monolayer deposited on the Indium Tin Oxide (ITO) glass surface, the ITO were treated with APTES (0.2 mmol·L⁻¹) in 10 mL toluene at 110 °C for 2 h under argon.

Synthesis of ZIF-90 membrane

The membrane of ZIF-90 was prepared by Zn(NO₃)₂·6H₂O and ICA in DMF based on the original literature. The ITO glasses treated by APTES were then placed in a stainless steel autoclave which was

filled with the above solution, and heated at 100 °C in air oven for 18 h. After solvothermal reaction, the ZIF-90 membrane was washed with DMF three times, and then dried in air at 60 °C over a night.

Physical measurements The powder X-ray diffraction (PXRD) patterns were recorded at room temperature under ambient conditions with Bruker D8 VANDANCE X-ray diffractometer with CuK α radiation under 40 kV and 40 mA, the data were collected within the 2 θ range of 5 - 60°. The UV-vis absorption spectra were obtained on an Agilent 8453 UV-vis spectrometer in the range of 190-1100 nm and the wavelength resolution of the instrument is 1 nm. The UV-vis absorption spectra were recorded using fine suspensions of powder samples (ZIF-90) and the different anions solution (F⁻, Cl⁻, Br⁻, I⁻, NO₃⁻, CO₃²⁻, C₂O₄²⁻ and CrO₄²⁻) with deionized water as dispersing solvent. In a general experiment, 4 mg of powder sample was suspended in 3 mL of deionized water in an ultrasonic bath for 5 min. The suspension was transferred to a 10 mm path length quartz cuvette to record the spectra. And the UV-vis absorption spectra of different anions were recorded with a series of a certain concentration of solutions. Scanning electronic microscope (SEM) images were recorded with a Hitachi S-4800 with a cold field emission gun operating at 2 kV and 10 μ A. TGA/DSC data were obtained on a STA449C (NETZSCH) instrument with a heating rate of 5 °C min⁻¹ under Ar atmosphere. Fourier transform infrared (FTIR) spectra were measured within the 4000-400 cm⁻¹ region on a Nexus 912 AO446 spectrophotometer with the KBr pellet technique. Photoluminescence spectra and luminescence lifetimes (τ) were detected by an Edinburgh FLS920 phosphorescent instrument. The fluorescence spectra were corrected for variations in the output of the excitation source (a 450 W xenon lamp) and for variations in the detector response. The excitation wavelength was 467 nm. The width of the excitation slit was 2 nm and the emission slit was 2 nm (wavelength resolution is 1 nm).

Conclusions

In summary, we prepared a zeolitic imidazolate framework (ZIF-90), which exhibits an intensive blue luminescence excited under visible light. As a luminescent material, ZIF-90 has multifunctional sensitivity to detect metal ions, anions and small molecules. Our study data indicate that the luminescence intensity of ZIF-90 is highly sensitive to Cd²⁺ and Cu²⁺ ions owing to the interaction with imidazole nitrogen sites of organic ligand. And the CrO₄²⁻ anions and small molecules such as acetone have the competition of absorption with ICA. The luminescence intensity of desolvated ZIF-90 increases proportionally to the concentration of Cd²⁺ but decreases proportionally to the concentration of Cu²⁺, and decreases with the increase of CrO₄²⁻ anions and acetone into the emulsions of ZIF-90a. This studies show that the ZIF-90 could be a useful luminescent sensor for metal ions, anions and organic small molecules. In subsequent study, ZIF-90 will have the wide application in gas detection and fluorescence test paper. This opens up a way that use a chemically and thermally stable MOFs as hosts to build some highly sensitive sensor with multifunction applications.

Acknowledgements

This work was supported by the National Natural Science Foundation of China (91122003) and the Developing Science Funds of Tongji University.

Notes and references

^a Department of Chemistry, Tongji University; Siping Road 1239, Shanghai 200092, China. Tel: +86-21-65984663; E-mail: byan@tongji.edu.cn

Electronic Supplementary Information (ESI) available: [details of any supplementary information available should be included here]. See DOI: 10.1039/b000000x/

- O. M. Yaghi, M. O'Keeffe, N. W. Ockwig, H. K. Chae, M. Eddaoudi and J. Kim, *Nature*, 2003, **423**, 705; S. Horike, S. Shimomura and S. Kitagawa, *Nat. Chem.*, 2009, **1**, 695.
- L. J. Li, S. F. Tang, C. Wang, X. X. Lv, M. Jiang, H. Z. Wu and X. B. Zhao, *Chem. Commun.*, 2014, **50**, 2304; F. Gandara, H. Furukawa, S. Lee and O. M. Yaghi, *J. Am. Chem. Soc.*, 2014, **136**, 5271; Y. L. Wang, C. H. Tan, Z. H. Sun, Z. Z. Xue, Q. L. Zhu, C. J. Shen, Y. H. Wen, S. M. Hu, Y. Wang, T. L. Sheng and X. T. Wu, *Chem. Eur. J.*, 2014, **20**, 1341.
- Y. B. He, W. Zhou, G. D. Qian and B. L. Chen, *Chem Soc Rev*, 2014, **43**, 5657; S. Roy, A. Chakraborty and T. K. Maji, *Coord. Chem. Rev.*, 2014, **273**, 139; S. L. Qiu, M. Xue and G. S. Zhu, *Chem. Soc. Rev.*, 2014, **43**, 6116.
- A. Misale, S. Niyomchon, M. Luparia and N. Maulide, *Angew Chem. Int. Ed.*, 2014, **53**, 7068; K. Manna, T. Zhang and W. B. Lin, *J. Am. Chem. Soc.*, 2014, **136**, 6566.
- M. Kurmoo, *Chem Soc Rev*, 2009, **38**, 1353.
- K. Jayaramulu, R. P. Narayanan, S. J. George and T. K. Maji, *Inorg. Chem.*, 2012, **51**, 10089; Z. M. Hao, X. Z. Song, M. Zhu, X. Meng, S. N. Zhao, S. Q. Su, W. T. Yang, S. Y. Song and H. J. Zhang, *J. Mater. Chem. A*, 2013, **1**, 11043; L. E. Kreno, K. Leong, O. K. Farha, M. Allendorf, R. P. Van Duyne and J. T. Hupp, *Chem. Rev.*, 2012, **112**, 1105; D. X. Ma, B. Y. Li, X. J. Zhou, Q. Zhou, K. Liu, G. Zeng, G. H. Li, Z. Shi and S. H. Feng, *Chem. Commun.*, 2013, **49**, 8964.
- Z. Z. Lu, R. Zhang, Y. Z. Li, Z. J. Guo and H. G. Zheng, *J. Am. Chem. Soc.*, 2011, **133**, 4172; Z. C. Hu, B. J. Deibert and J. Li, *Chem Soc Rev*, 2014, **43**, 5815; B. Li, X. Chen, F. Yu, W. J. Yu, T. L. Zhang and D. Sun, *Cryst. Growth Des.*, 2014, **14**, 410.
- P. Vineis, G. Hoek, M. Krzyzanowski, F. Vigna-Taglianti, F. Veglia, L. Airoidi, K. Overvad, O. Raaschou-Nielsen, F. Clavel-Chapelon, J. Linseisen, H. Boeing, A. Trichopoulou, D. Palli, V. Krogh, R. Tumino, S. Panico, H. B. Bueno-De-Mesquita, P. H. Peeters, E. Lund, A. Agudo, C. Martinez, M. Dorransoro, A. Barricarte, L. Cirera, J. R. Quiros, G. Berglund, J. Manjer, B. Forsberg, N. E. Day, T. J. Key, R. Kaaks, R. Saracci and E. Riboli, *Environ Health-Uk*, 2007, **6**; M. Kampa and E. Castanas, *Environ. Pollut.*, 2008, **151**, 362; J. L. Martinez, *Environ. Pollut.*, 2009, **157**, 2893.
- C. P. Han and H. B. Li, *Anal. Bioanal. Chem.*, 2010, **397**, 1437.
- X. Y. Xu and B. Yan, *ACS Appl. Mater. Interfaces*, 2015, **7**, 721.
- J. N. Hao and B. Yan, *J. Mater. Chem. A*, 2014, **2**, 18018.
- Y. Zhou and B. Yan, *Inorg. Chem.*, 2014, **53**, 3456.
- T. W. Duan and B. Yan, *J. Mater. Chem. C*, 2014, **2**, 5098.

- 14 B. L. Chen, Y. Yang, F. Zapata, G. N. Lin, G. D. Qian and E. B. Lobkovsky, *Adv. Mater.*, 2007, **19**, 1693; B. L. Chen, L. B. Wang, F. Zapata, G. D. Qian and E. B. Lobkovsky, *J. Am. Chem. Soc.*, 2008, **130**, 6718; F. Liu, B. Chen, B. Glettner, M. Prehm, M. K. Das, U. Baumeister, X. Zeng, G. Ungar and C. Tschierske, *J. Am. Chem. Soc.*, 2008, **130**, 9666.
- 15 C. Q. Zhang, L. B. Sun, Y. Yan, J. Y. Li, X. W. Song, Y. L. Liu and Z. Q. Liang, *Dalton Trans.*, 2015, **44**, 230.
- 16 S. Liu, Z. H. Xiang, Z. Hu, X. P. Zheng and D. P. Cao, *J. Mater. Chem.*, 2011, **21**, 6649.
- 17 X. Peng, X. Cheng and D. P. Cao, *J. Mater. Chem.*, 2011, **21**, 11259; B. L. Chen, L. B. Wang, Y. Q. Xiao, F. R. Fronczek, M. Xue, Y. J. Cui and G. D. Qian, *Angew. Chem. Int. Edi.*, 2009, **48**, 500.
- 18 K. S. Park, Z. Ni, A. P. Cote, J. Y. Choi, R. D. Huang, F. J. Uribe-Romo, H. K. Chae, M. O'Keeffe and O. M. Yaghi, *Proc. Natl. Acad. Sci. U. S. A.*, 2006, **103**, 10186.
- 19 W. Morris, C. J. Doonan, H. Furukawa, R. Banerjee and O. M. Yaghi, *J. Am. Chem. Soc.*, 2008, **130**, 12626.
- 20 T. Jiang, Y. F. Zhao and X. M. Zhang, *Inorg. Chem. Commun.*, 2007, **10**, 1194; G. Tian, G. S. Zhu, Q. R. Fang, X. D. Guo, M. Xue, J. Y. Sun and S. L. Qiu, *J. Mol. Struct.*, 2006, **787**, 45; H. Y. Bai, J. F. Ma, J. Yang, L. P. Zhang, J. C. Ma and Y. Y. Liu, *Cryst Growth Des*, 2010, **10**, 1946; S. W. Thomas, G. D. Joly and T. M. Swager, *Chem. Rev.*, 2007, **107**, 1339.
- 21 Z. F. Xin, X. S. Chen, Q. Wang, Q. Chen and Q. F. Zhang, *Micropor. Mesopor. Mater.*, 2013, **169**, 218-221.
- 22 Y. Lu and B. Yan, *Chem. Commun.*, 2014, **50**, 13323.
- 23 A. S. Huang, W. Dou and J. Caro, *J. Am. Chem. Soc.*, 2010, **132**, 15562.